



Lightweight CIGS2 Thin-Film Solar Cells on Stainless Steel Foil

Authors

Dhere, Neelkanth G.
Ghongadi, Shantinath R. and
Pandit, Mandar B.

Presented At:

17th European Photovoltaic Solar Energy Conference
Munich, Germany, 22-26 October 2001

Publication Number

FSEC-PF-427-01

Copyright

Copyright © Florida Solar Energy Center/University of Central Florida
1679 Clearlake Road, Cocoa, Florida 32922, USA
(321) 638-1000
All rights reserved.

Disclaimer

The Florida Solar Energy Center/University of Central Florida nor any agency thereof, nor any of their employees, makes any warranty, express or implied, or assumes any legal liability or responsibility for the accuracy, completeness, or usefulness of any information, apparatus, product, or process disclosed, or represents that its use would not infringe privately owned rights. Reference herein to any specific commercial product, process, or service by trade name, trademark, manufacturer, or otherwise does not necessarily constitute or imply its endorsement, recommendation, or favoring by the Florida Solar Energy Center/University of Central Florida or any agency thereof. The views and opinions of authors expressed herein do not necessarily state or reflect those of the Florida Solar Energy Center/University of Central Florida or any agency thereof.

LIGHTWEIGHT CIGS2 THIN-FILM SOLAR CELLS ON STAINLESS STEEL FOIL

Neelkanth G. Dhere, Shantinath R. Ghongadi and Mandar B. Pandit
Florida Solar Energy Center
1679 Clearlake Road, Cocoa, FL 32922-5703, USA
Phone: (407) 638-1442, Fax: (407) 638-1010, e-mail: dhere@fsec.ucf.edu

ABSTRACT: AM 0 PV parameters of large-grain, {112} orientated chalcopyrite CIGS2 thin films solar cells on 127 μm thick SS flexible foil for space power were: $V_{oc} = 802.9$ mV, $J_{sc} = 25.07$ mA/cm², FF = 60.06%, and efficiency 0 = 8.84%. Detailed current versus voltage analysis gave values of series resistance R_s , shunt resistance R_p , diode factor A, and reverse saturation current J_0 of ~ 0.1 Ω cm², ~ 600 Ω cm², ~ 2.2 and $\sim 1.85 \times 10^{-8}$ A cm⁻² respectively. A sharp QE cutoff was observed at CIGS2 bandgap of ~ 1.50 eV. Higher foil roughness resulted in a preliminary low 4.06% (AM 1.5) efficiency of CIGS2 solar cell on 20 μm thick SS foil. Present specific power of 65 W/kg can be increased by over 10 times with 10% AM 0 CIGS cells on 20-25 μm thick SS or Ti foils.

Keywords: CIGS2 solar cells- 1: SS Foil - 2: Light weight

1. INTRODUCTION

The purpose of this research is to develop $\text{CuIn}_{1-x}\text{Ga}_x\text{S}_2$ (CIGS2) thin-film solar cells on flexible stainless steel (SS) foils for space power. CIGS2 thin-film solar cells are of interest for space power applications because of the near optimum bandgap for AM0 solar radiation in space [1-7]. $\text{CuIn}_{1-x}\text{Ga}_x\text{Se}_{2-y}\text{S}_y$ (CIGS) and CIGS2 solar cells are expected to be superior to Si and GaAs solar cells for space missions especially in terms of the performance at the end of low earth orbit (LEO) missions [8,9]. CIGS2 thin film solar cells on flexible SS may be able to increase the specific power by an order of magnitude from the current level of 65 Wkg⁻¹. Thin-film technology could conservatively reduce the array-manufacturing cost of medium-sized five-kilowatt satellite from the current level of \$2000k to less than \$500k [10]. Preparation and properties of CIGS thin-film solar cells deposited on glass substrates have been described in earlier studies [11,12]. This paper presents preparation and detailed photovoltaic (PV) characterization of CIGS2 thin-film solar cells on SS flexible foil substrates for ultra-lightweight space solar power.

2. EXPERIMENTAL TECHNIQUE

DC-magnetron-sputtering parameters for deposition of molybdenum back-contact layer were optimized so as to minimize the residual stresses developed during deposition. Bright annealed stainless steel foils of thicknesses 127 μm and 20 μm were evaluated as possible substrate materials for polycrystalline CIGS2 solar cell. Crystalline phases, surface morphology, and composition-depth profile of CIGS2 films deposited on SS flexible foils substrates were studied by X-ray diffraction (XRD) and scanning electron microscopy (SEM).

Approximately 40%-Cu-rich Cu-Ga/In layers were sputter-deposited on unheated Mo-coated SS foils from

CuGa(22%) and In targets. Well-adherent, large-grain Cu-rich CIGS2 films were obtained by sulfurization in an Ar:H₂S 1:0.04 mixture at argon flow rate of 650 sccm and the maximum temperature of 475° C for 60 minutes with intermediate 30 minute annealing step at 135° C. p-type CIGS2 thin films were obtained by etching away the Cu-rich layer segregated at the surface in dilute (10%) KCN solution for 3 minutes [13,14]. Solar cells were completed by deposition of CdS heterojunction partner layer by chemical bath deposition, transparent-conducting ZnO/ZnO:Al window bilayer by RF sputtering, and vacuum deposition of Ni/Al contact fingers through metal mask [15]. PV parameters of the best solar cell on SS foil were measured under AM 0 and AM 1.5 conditions at the NASA Glenn Research Center (GRC) and National Renewable Energy Laboratory respectively. Detailed PV characteristics were obtained at the Institute of Energy Conversion (IEC) [6,11].

3. RESULTS AND DISCUSSION

Surface roughness of SS foil substrates was measured using DEKTAK³ surface profile measuring system. In case of 127 μm thick SS foil, the average roughness (R_a) was 62.3 Å and average waviness (W_a) was 141.6 Å. The average roughness and average surface waviness were respectively 396.4 Å and 773.2 Å for the 20 μm thick SS foil. XRD and SEM analysis of a CIGS2 film on SS foil revealed growth of large (~ 3 μm), compactly-packed, faceted grains of chalcopyrite CIGS2 phase having $a_0 = 5.519$ X and $c_0 = 11.125$ X and {112} preferred orientation. SIMS depth profile of CIGS2 film showed gallium concentration increasing toward the back contact.

PV parameters of the best CIGS2 solar cell on 127 μm thick SS flexible foil measured under AM 0 conditions at the NASA Glenn Research Center were: $V_{oc} = 802.9\text{ mV}$, $J_{sc} = 25.07\text{ mA/cm}^2$, $FF = 60.06\%$, and $\theta = 8.84\%$. For this cell, AM 1.5 PV parameters measured at NREL were: $V_{oc} = 788\text{ mV}$, $J_{sc} = 19.78\text{ mA/cm}^2$, $FF = 59.44\%$, $\theta = 9.26\%$.

Results of the detailed PV characteristics consisting of the analysis of short circuit current, J versus voltage, V and quantum efficiency data obtained at IEC for this cell are presented in the following. The J - V characteristics in light and dark were compared to verify if the light characteristic was essentially a translated curve with light short circuit current, J_{sc} or J_L (Figure 1). There was slight crossover at current densities over $1.9 \times J_{sc}$ indicating a moderately photoconducting heterojunction partner layer.

J - V characteristics under illumination provided J_{sc} , V_{oc} , FF , and θ , in addition to R_s , R_p . Ascending and descending curves showed hysteresis. The main part of $\log(J+J_{sc})$ versus V_t curves showed diode behavior (Figure 2). The offset between dark and light curves is attributed to the higher reverse saturation current, J_0 under illumination. The curve is affected by the shunt resistance, R_p at low voltages. In the present cell, shunting effects became predominant below 0.1 mA cm^{-2} . Usually, slopes are modified due to series resistance at very high currents. In the present case, series resistance effect was not observed even at $\sim 59\text{ mA cm}^{-2}$ i.e. $\sim 3 \times J_{sc}$.

The dJ/dV versus V curve measures ac conductance around J_{sc} (Figure 3). For the dark curve, it gave a reasonable value of $600\ \Omega\text{ cm}^2$ for the shunt resistance, R_p . The light curve showed a slight change of collection with voltage. The un-smoothed light curve was noisy due to flicker in xenon arc lamp. The scatter was reduced by using values of dJ/dV calculated by the nine-point differential method. dV/dJ versus $1/J+J_{sc}$ curve was plotted

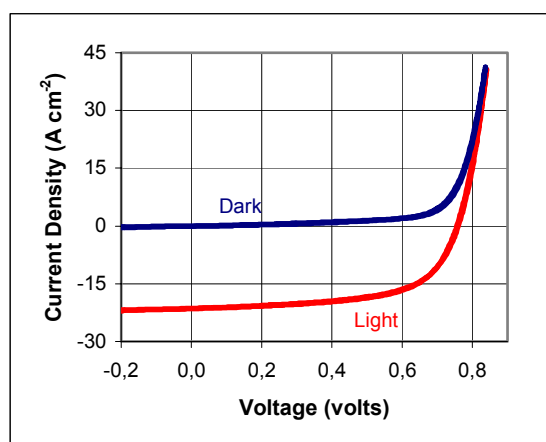


Fig. 1. Variation of light and dark current densities with voltage

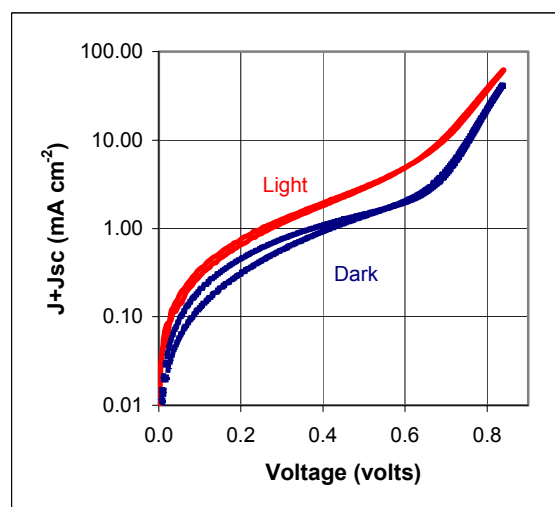


Fig. 2. $\log(J+J_{sc})$ versus total voltage V_t curves

to estimate ac resistance in forward bias. The straight lines show diode or exponential behavior (Figure 4). The intercept at ∞ current gave a very low value of series resistance, R_s of $\sim 0.1\ \Omega\text{ cm}^2$. It can be seen that there is moderate hysteresis. It indicates non-coincidence between ascending and descending curves. Values of the diode factor, A and reverse saturation current density, J_0 can be obtained from a plot of natural logarithm of $(J+J_{sc})$ versus corrected voltage V' i.e. $(V-R_sJ)$. Figure 5 shows a plot of the diode factor, A and reverse saturation current,

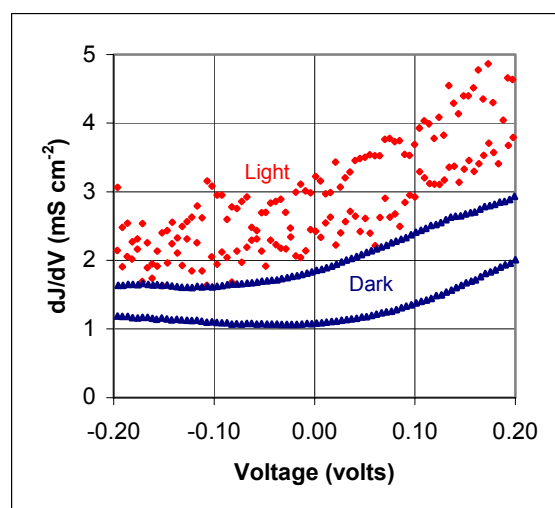


Fig. 3. dJ/dV versus voltage characteristics

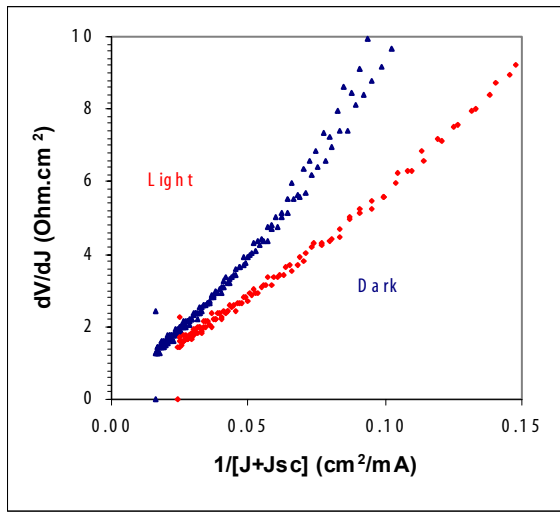


Fig. 4. Variation of dV/dJ with $1/J+J_{sc}$

J_0 versus $\ln J$ (dark). Values of diode factor, A and reverse saturation current, J_0 can be seen to vary respectively around ~ 2.21 and $\sim 1.85 \times 10^{-8}$ $A\ cm^{-2}$ over a wide range of current densities.

Quantum efficiency (QE) curves were obtained in the dark and under AM1 light illumination, without bias ($V = 0$) and with reverse ($-0.5\ V$) and forward ($0.5\ V$) bias (Figure 6). They showed only a modest loss at high energy by the thin heterojunction partner CdS layer. At

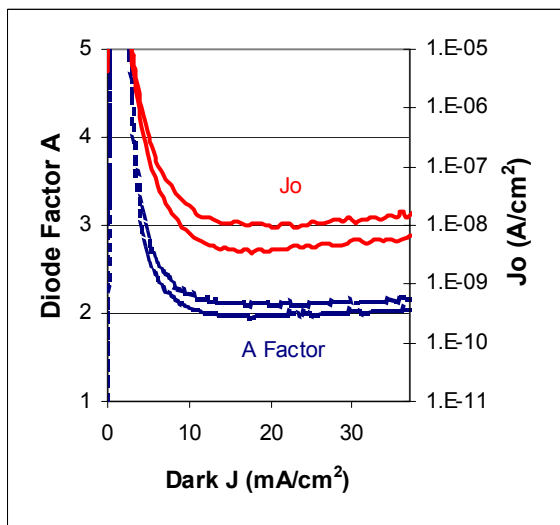


Fig. 5. Variation of diode factor, A , and reverse saturation current density, J_0 , with the dark current density, J .

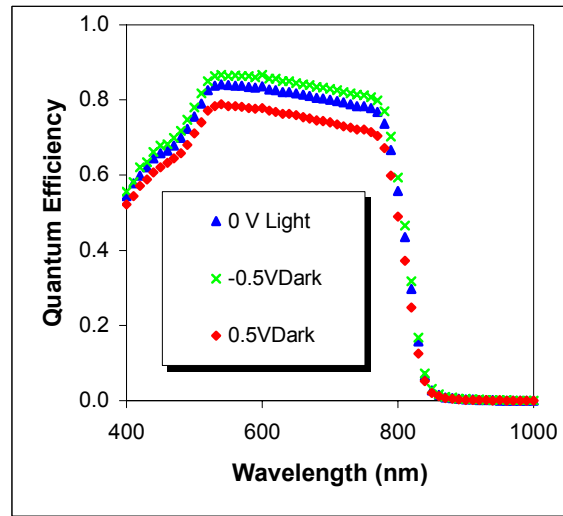


Fig. 6. Variation of quantum efficiency with wavelength.

low energy, a sharp QE cutoff was observed equivalent to CIGS2 bandgap of $\sim 1.50\ eV$.

Another set of curves was obtained for normalized QE versus photon energy in electron-volt, eV . For this purpose, the peak value of each curve was normalized to 1. At low energies, the curves showed almost no difference in collection and a QE cut off at $\sim 1.50\ eV$. Unbiased samples showed CdS absorption at high energies. Detailed PV characterization consisting of the analysis of short circuit current, J versus voltage, V and quantum efficiency data showed that CIGS2 thin film solar cells on SS substrates were normal without serious limitations and with promising characteristics.

Preliminary experiments were carried out for preparation of CIGS2 solar cells on $20\ \mu m$ thick SS and $25.4\ \mu m$ thick titanium foils. PV parameters of an unoptimized cell fabricated on $20\ \mu m$ thick SS foil and measured at NREL under AM 1.5 conditions were: $V_{oc} = 740\ mV$, $J_{sc} = 13.129\ mA/cm^2$, $FF = 41.63\%$, efficiency $\eta = 4.06\%$. It may be noted that the average roughness (R_a) of $20\ \mu m$ thick SS foil was $396.4\ \text{\AA}$ while that of $127\ \mu m$ was $62.3\ \text{\AA}$. The loss of efficiency is attributed to surface roughness. It is expected that when smoother $20\ \mu m$ SS foil become available, it would be possible to prepare CIGS2 or CIGS solar cells with AM 0 efficiency in the range of 10 to 15%. Table I provides the projected specific power in W/Kg of flexible metallic substrate for 10 and 15% AM 0 efficient CIGS2 solar cells. Thus it can easily be seen that even 10% AM 0 CIGS cells on thin SS or Ti foils will increase the specific power by over an order of magnitude from the present value of $65\ W/kg$ [16].

Table I. Projected Specific Power in W/Kg.

Substrate Thicknes Material	Projected Specific Power in W/Kg	
	AM 0 $\eta = 10\%$	AM 0 $\eta = 15\%$
127- μm (5 mil) SS foil	133	200
20- μm (< 1mil) SS foil	769	1153
25.4- μm (1 mil) Ti foil	1016	1524

5. CONCLUSIONS

Preparation parameters were optimized to obtain large ($\sim 3 \mu\text{m}$), compactly-packed, faceted-grain, CIGS2 thin films on SS flexible foil with {112} preferred orientation of chalcopyrite phase having $a_0 = 5.519 \text{ X}$ and $c_0 = 11.125 \text{ X}$. AM 0 PV parameters of a CIGS2 solar cell on 127 μm SS flexible foil were: $V_{oc} = 802.9 \text{ mV}$, $J_{sc} = 25.07 \text{ mA/cm}^2$, $FF = 60.06\%$, and $\theta = 8.84\%$. Detailed J-V analysis gave values of series resistance R_s , shunt resistance R_p , diode factor A, and reverse saturation current J_0 , of $\sim 0.1 \Omega \text{ cm}^2$, $\sim 600 \Omega \text{ cm}^2$, ~ 2.2 and $\sim 1.85 \times 10^{-8} \text{ A cm}^{-2}$ respectively. Quantum efficiency curve showed a sharp QE cutoff equivalent to CIGS2 bandgap of $\sim 1.50 \text{ eV}$, fairly close to the optimum value for efficient AM0 PV conversion in the space. Low 4.06% (AM 1.5) efficiency of an un-optimized CIGS2 solar cell on 20 μm thick SS foil is attributed to higher foil roughness. Calculations show that even 10% AM 0 CIGS cells on 20-25 μm thick SS or Ti foils will increase the specific power by over 10 times from the present value of 65 W/kg.

ACKNOWLEDGEMENTS

This work was supported by the National Renewable Energy Laboratory (NREL) and the NASA Glenn Research Center. The authors are thankful to Dr. William A. Shafarman of Institute of Energy Conversion, University of Delaware, for J-V and QE measurements and discussions, David Scheiman of Ohio Aerospace Institute for AMO measurements, and Dr. Kannan Ramnathan of NREL for help with Ni/Al grid deposition and discussions.

REFERENCES

- [1] D. J. Flood, Prog. Photovolt. Res. Appl. **6** (1998) 187-192.
- [2] S. G. Bailey and D. J. Flood, Prog. Photovolt. Res. Appl. **6** (1998) 1-14.
- [3] N. G. Dhere, S. R. Ghongadi, M. B. Pandit, and A. H. Jahagirdar, Proc. 17th NASA Space Power Conference (SPRAT), Cleveland, Ohio, 2001.
- [4] N. G. Dhere and S. R. Ghongadi, Mat. Res. Soc. Symp. Proc. **668** (2001) H3.4.1-H3.4.6.
- [5] N. G. Dhere, S. R. Kulkarni, and P. K. Johnson, Proc. 16th European Photovoltaic Solar Energy Conference, Glasgow, UK, (2000) 978-981.
- [6] N. G. Dhere, S. R. Kulkarni and S. R. Ghongadi, PV characterization of CIGS2 thin film solar cells, 28th IEEE Photovoltaic Specialists Conference, Anchorage, Alaska, (2000) 1046-1049.
- [7] N. G. Dhere, S. R. Kulkarni, S. S. Chavan and S. R. Ghongadi, Proc. NASA Space Power Conference (SPRAT), Cleveland, Ohio, (1999).
- [8] S. Messenger, R. Walters, G. Summers, T. Morton, G. La Roche, C. Signorini, O. Anzawa, and S. Matsuda, Proc. 16th European Photovoltaic Solar Energy Conference, Glasgow, UK, (2000) 974-977.
- [9] A. Boden, D. Br̄unig, J. Klaer, F. H. Karg, B. H̄sselbarth, G. La Roche, Proc. 28th IEEE Photovoltaic Specialists Conference, Anchorage, Alaska, (2000) 1038-1041.
- [10] J. Tringe, J. Merrill, and K. Reinhardt, Proc. 28th IEEE Photovoltaic Specialists Conference, Anchorage, Alaska, (2000) 1242-1245.
- [11] N. G. Dhere, S. Kuttath, K. W. Lynn, R. W. Birkmire, and W. N. Shafarman, Proc. 1st World Conf. Photovoltaic Solar Energy Conf., Hawaii, (1994) 190-193.
- [12] N. G. Dhere, S. Kuttath, and H. R. Moutinho, J. Vac. Sci. & Technol. A **13** (1995) 1078-1082.
- [13] R. Scheer, Trends in Vac. Sci. & Technol. **2** (1997) 77-112.
- [14] J. Klaer, J. Bruns, R. Henninger, K. T̄pper, R. Klenk, K. Ellmer and D. Br̄unig, Proc. 2nd World Conf. Photovoltaic Solar Energy Conf., Vienna, (1998) 537-540.
- [15] K. Ramanathan, F. S. Hasoon, H. Al-Thani, J. Alleman, J. Keane, J. Dolan, M. A. Contreras, R. Bhattacharya and R. Noufi, Proc. NCPV Program Rev. Meeting, Lakewood, CO, (2001) 45-48.
- [16] J. R. Tuttle, A. Szalaj and J. Keane, Proc. 28th IEEE Photovoltaic Specialists Conference, Anchorage, Alaska, (2000), 1042-1045.